

Photogating of mono- and few-layer MoS₂

Bastian Miller, Eric Parzinger, Anna Vernickel, Alexander W. Holleitner, and Ursula Wurstbauer
*Walter Schottky Institut and Physik-Department,
 Technische Universität München, 85748 Garching, Germany and
 Nanosystems Initiative Munich (NIM), Schellingstr. 4, 80799 München, Germany*
 (Dated: March 3, 2015)

We describe a photogating effect in mono- and few-layer MoS₂, which allows the control of the charge carrier density by almost two orders of magnitude without electrical contacts. Our Raman studies are consistent with physisorbed environmental molecules, that effectively deplete the intrinsically n-doped charge carrier system via charge transfer, and which can be gradually removed by the exposure to light. This photogating process is reversible and precisely tunable by the light intensity. The photogating efficiency is quantified by comparison with measurements on electrostatically gated MoS₂.

Two-dimensional layered van-der Waals materials and their heterostructures, particularly the transition metal dichalcogenides (TMDCs) family such as MoS₂, are of great interest for fundamental research as well as for novel device concepts in the areas of electronic [1, 2], optoelectronic [1, 3–5], valley- and spintronic [6] as well as solar energy conversion [7] and sensing applications [8]. It has been demonstrated that MoS₂ undergoes a transition from an indirect to a direct bandgap semiconductor by thinning it down to one single layer [3]. The direct gap at the *K*-point with $E_{gap} = 1.9$ eV [3] remains almost unaffected by the number of layers. The indirect gap existing in vicinity of the Γ -point decreases in energy for increasing number of layers [3]. In particular, a high absorption of the monolayer of 5-10% in the visible regime [9] makes MoS₂ a promising material for optoelectronic devices such as phototransistors and solar cells. For atomistic thin materials, knowledge about the interaction with the dielectric environment is of great importance. The impact of substrates [10, 11], the gaseous environment as well as of adsorbates [12–14] on the optoelectronic properties of 2D materials have been reported. The atomistic interfaces offer the opportunity of novel route for interfacial engineering of electronic, optical and optoelectronic properties [10, 12, 15, 16].

In this letter, we study the effect of photogating in MoS₂ mono- and few-layer flakes by means of Raman spectroscopy. Our observations are consistent with physisorbed environmental molecules acting as molecular gates. The molecules can be gradually removed from the MoS₂ surface by the exposure to light. We find that the photogating effect facilitates the control of the charge carrier density in MoS₂ by almost two orders of magnitude in pristine flakes without the need for electrical contacts. In general, Raman spectroscopy provides access to various properties of 2D layered materials [17] such as to the number of layers [18, 19], to strain [20, 21] to the local temperature [22] and to the doping level [23]. The Raman spectrum of MoS₂ includes two prominent first-order phonon modes, the E_{2g}^1 and the A_{1g} mode [17]. The E_{2g}^1 mode is an in-plane mode, i.e. the atoms are oscillating parallel to the basal plane of the van-der Waals coupled crystal layers. The A_{1g} mode is an out-of plane

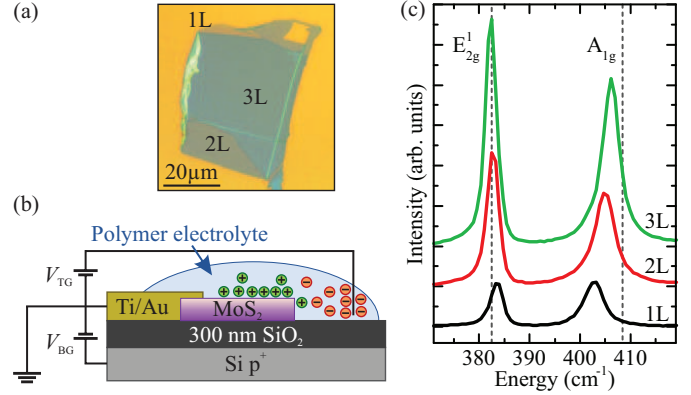


FIG. 1. (a) Optical microscopy image (100x) of a MoS₂ flake exhibiting mono-, bi- and tri-layer areas. (b) Scheme of a top- and back-gated MoS₂ field-effect device for optical measurements. (c) Raman spectra of mono-, bi-, tri-layer areas of the MoS₂ flake shown in (a). The dashed lines mark the phonon energies for bulk MoS₂.

oscillation, where the sulfur atoms are moving in opposite directions. Raman studies on mono- and few-layer MoS₂ reveal, that the energy of the E_{2g}^1 mode decreases with increasing number of layers, whereas the energy of the A_{1g} mode increases with the number of layers [18]. Moreover, it has been reported for a monolayer of MoS₂ that the energy of the A_{1g} mode is sensitive to the doping level due to phonon renormalization [23].

In our experiments, laser power dependent Raman spectra taken on pristine mono- and few-layers of MoS₂ on Si/SiO₂ and sapphire substrates in ambient conditions and vacuum are contrasted with Raman measurements taken on electrostatically doped MoS₂ utilizing a field-effect device on SiO₂ substrate. For mono- bi-, tri- and four-layer flakes, we find a laser power induced shift of the A_{1g} phonon mode energy. From a comparison with measurements done on electrostatically gated mono- and bilayer MoS₂ devices, we interpret the light induced shift as a change in the charge carrier density Δn via a photogating effect. We further find that for up to 4 layers, the photogating effect scales linearly to the inverse number

of layers. Therefrom, we conclude that the free charge carriers are delocalized and homogeneously distributed over all layers for all investigated samples. The observed photogating effect is not persistent, not observable in vacuum and independent from the investigated substrates. The photogating effect is of importance for future mono- and few-layered MoS₂ optoelectronic devices operating in ambient conditions.

The studied MoS₂ flakes are micromechanically exfoliated from naturally occurring bulk crystals. They are transferred on sapphire or Si/SiO₂ substrates [Fig. 1(a)]. The latter consists of p⁺-doped silicon with a 300 nm thick SiO₂ layer [Fig. 1(b)]. All flakes are characterized by optical microscopy [Fig. 1 (a)] and μ -Raman spectroscopy in back scattering geometry under ambient conditions at room temperature with $\lambda = 488$ nm [Fig. 1(c)]. The power of the exciting laser is varied from 25 to 1000 μ W resulting in a power density between 0.5 kW/cm² and 56.6 kW/cm². Ohmic contacts for the dual gated MoS₂ field-effect device [Fig. 1(b)], are prepared by optical lithography and e-beam evaporation of Ti/Au (5 nm/20 nm). The doped Si substrate serves as a back gate electrode. A solid polymer electrolyte (PE) composed of a mixture of polyethylene-oxide and CsClO₄ act as a transparent top gate electrode [24]. The capacity of such an electrode is as high as $C_{TG} \approx 1.5$ μ F/cm² [23] providing a charge injection parameter of $\alpha_{PE} \approx 0.9 \times 10^{13}$ cm⁻²/V. The MoS₂ flakes are intrinsically n-type doped as confirmed from complementary electrical measurements on a field-effect transistor device (data not shown).

The Raman spectra of the MoS₂ flake depicted in Fig. 1(a) are shown for the mono-, bi- and tri-layer areas in Fig. 1(c). The energies of the E_{2g}^1 and the A_{1g} modes as well as their energy difference $\Delta E = |E_A - E_E|$ are in excellent agreement to reported values in literature [18]. We note that for the field-effect device, the energy of the A_{1g} phonon is red shifted by about 0.6 cm⁻¹ after deposition of the PE top gate. We ascribe this shift to a moderate modification of the charge carrier density in MoS₂ introduced from a different dielectric environment on the top interface by adding the PE. The E_{2g}^1 mode is unaffected by the presence of the PE electrode within the experimental error of ± 0.2 cm⁻¹. This excludes strain to be introduced by the polymer film covering the MoS₂ flake [20].

Fig. 2 shows Raman spectra in dependence of the laser power of pristine monolayer MoS₂ on SiO₂ and on sapphire in ambient conditions as well as on SiO₂ in vacuum [Figs. 2(a,c,e)]. For the measurements performed in ambient conditions [Figs. 2(a,e)], the A_{1g} mode shifts towards lower energies. Furthermore, it broadens with increasing laser power, while the E_{2g}^1 mode remains almost unaffected. Figs. 2(b,d,f) show the energies of the A_{1g} and E_{2g}^1 modes vs. the laser power in a semi-logarithmic representation. Within the experimental resolution, an exponential dependence of the A_{1g} mode energy from the laser power is observable for all samples measured in am-

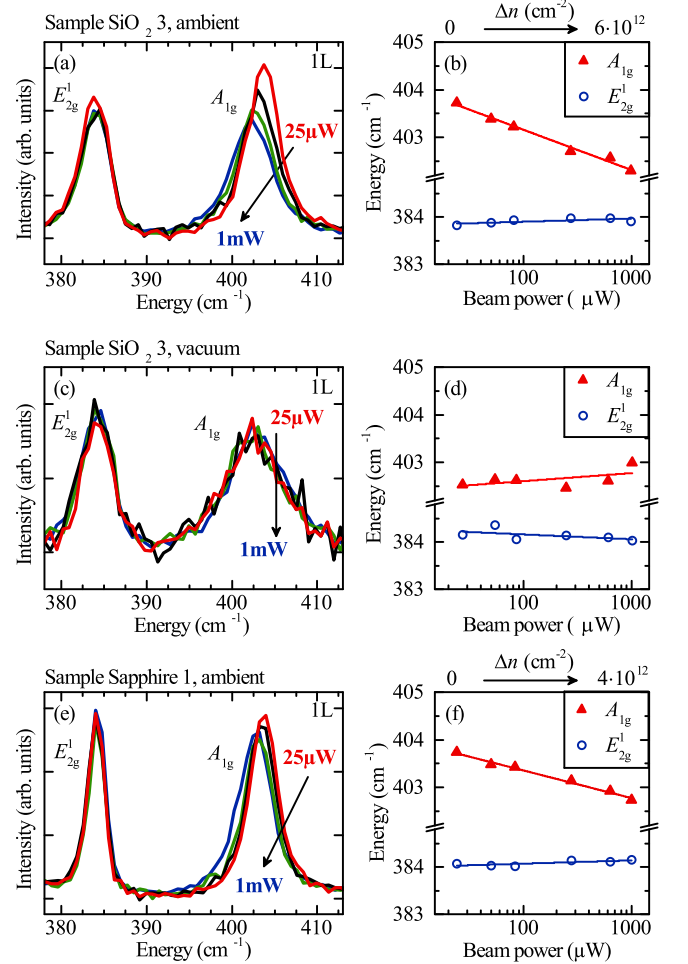


FIG. 2. Raman spectra of monolayer MoS₂ for different laser powers ranging from 25 to 1000 μ W (a) on Si/SiO₂ taken in ambient conditions, (c) on Si/SiO₂ in vacuum and (e) on sapphire in ambient. (b), (d), (f) Semi-logarithmic representation of the related A_{1g} and the E_{2g}^1 mode energies in dependence of the laser power. The solid lines are linear fits to the data points.

ambient conditions. The energy of the E_{2g}^1 phonon mode is unaffected by the laser power. Therefore, light-induced heating of the MoS₂ flake can be ruled out [22]. As discussed below, we attribute the redshift of the A_{1g} mode to a phonon renormalization by an increase of free charge carriers; consistent with earlier reports on an electrostatically doped monolayer MoS₂ [23].

To corroborate our interpretation, we perform complementary Raman studies on electrostatically gated MoS₂ mono- and bi-layer field-effect devices. Fig. 3 encloses that the A_{1g} mode energy is linearly dependent on the applied gate voltage and hence on the change in charge carrier density Δn for both MoS₂ mono- and bi-layer flakes. Again, the E_{2g}^1 mode is unaffected by the gate voltage within the experimental range. The gate induced change in the charge carrier density Δn can be quantified from the charge injection parameter α [top axes in Fig.

3]. Consequently, the light induced change Δn can be deduced from a direct comparison with gate-voltage dependent measurements [top axes in Figs. 2(b) and 2(f)]. With both methods, the charge carrier density can be tuned by almost two orders of magnitude identified by a shift of the A_{1g} phonon mode of $\approx 3 \text{ cm}^{-1}$ for mono- and $\approx 1.5 \text{ cm}^{-1}$ for bi-layers, respectively.

sample (environment)	E_A (cm^{-1})	FWHM (cm^{-1})	ΔE_A (cm^{-1})	Δn (10^{12}cm^{-2})
SiO ₂ 1 (a)	404.1	3.6	-0.6	2.8
SiO ₂ 1 (v)	402.6	5.9	0.0	< 0.1
SiO ₂ 2 (a)	404.3	3.3	-0.3	1.5
SiO ₂ 3 (a)	403.7	4.1	-1.4	6.0
SiO ₂ 3 (v)	402.5	7.0	0.0	<0.0
SiO ₂ 4 (a)	403.1	5.2	-2.3	10.0
Sapphire 1 (a)	403.7	3.6	-0.9	4.1
Sapphire 2 (v)	402.1	6.9	<-0.1	< 0.6

TABLE I. Energy E_A and full width at half maximum (FWHM) of the A_{1g} mode ($P = 25 \mu\text{W}$) measured in ambient (a) and vacuum (v) as a measure for the intrinsic charge carrier density. Photogating efficiency given by the decrease of the A_{1g} mode energy ΔE_A by increasing the power from $P = 25 \mu\text{W}$ to $P = 1 \text{ mW}$. ΔE_A has been translated into a change in the electron density Δn by comparison with electrostatic doping.

We note that the described photogating effect is not persistent and it is independent from the used substrate. It is reversible and tunable by the power of the light. Photogating is not observable for measurements in vacuum as shown exemplarily for MoS₂ on SiO₂ in Figs. 2 (c,d). These findings strongly suggest that the interface between MoS₂ and the gaseous environment causes the laser power dependent change in the charge carrier density Δn . Additionally, the A_{1g} mode is significantly broadened and red-shifted for measurements in vacuum with $p \leq 5 \times 10^{-6}$ mbar [Fig. 2 (c)] compared to measurements in ambient conditions. This behavior suggests a large charge carrier density of MoS₂ in vacuum, which is independent from the laser power [Fig. 2(d)]. The enhanced doping in vacuum is entirely reversible. After measurements in vacuum and exposing the MoS₂ sheets to ambient air, the A_{1g} mode is again stiffened and the FWHM is reduced. We further point out that the absolute values of the A_{1g} mode energy and FWHM vary from sample to sample (compiled for 6 samples in table I). However, the individual values are stable against repetition of measurements in vacuum and ambient conditions as well as measurements with varying light intensities.

We explain the photogating by a photodesorption of environmental molecules that are physisorbed on the MoS₂ surface. It has been reported in literature from photoluminescence measurements that physisorption of H₂O and O₂ molecules leads to a reduction of the charge carrier density in MoS₂ [12, 14]. The physisorbed

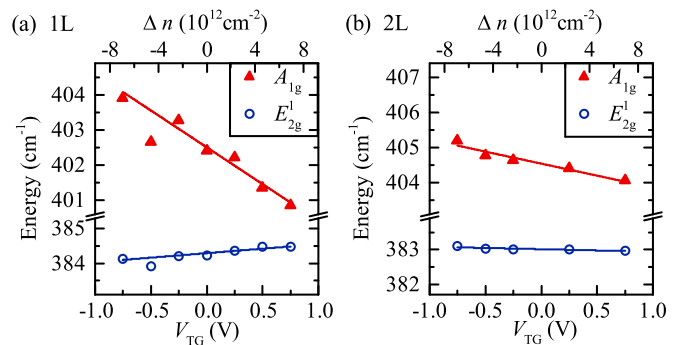


FIG. 3. Energy of the A_{1g} and the E_{2g}^1 modes in dependence of the applied top gate voltage for mono-layer (a) and bilayer MoS₂ (b). The solid lines are linear fits to the data points.

molecules act as molecular gates [12, 15] causing a charge transfer from the MoS₂ surface to the molecules of ≈ 0.01 electrons per H₂O molecule and ≈ 0.04 electrons per O₂ molecule [12, 14]. These values are for defect free crystals. The charge transfer from MoS₂ to molecules that are physisorbed on defect sites or wrinkles might be altered. Removing such molecules prevents the charge transfer from the MoS₂ layers resulting in an increasing charge carrier density. The binding energies of physisorbed H₂O and O₂ molecules on the surface of MoS₂ determined from density functional theory (DFT) calculations are 110 meV and 79 meV, respectively [12, 14]. Consistently, both molecules can be easily removed with measurements under high-vacuum conditions, especially during the exposure to light.

Let us now turn to the discussion of the laser power dependent increase of the charge carrier density for measurements in ambient conditions. We find a softening and broadening of the A_{1g} phonon mode for measurements performed in vacuum as well as for measurements under ambient conditions with a high laser power of $P = 1 \text{ mW}$. In line with the removal of a large amount of physisorbed molecules in vacuum, we interpret the laser power dependence of the A_{1g} mode as a consequence of laser induced cleaning of the MoS₂ surface. In this picture, an increase of the laser power diminishes the number of physisorbed molecules and hence, the charge transfer from MoS₂ to the molecules is reduced. In short, for a low laser power a larger amount of physisorbed environmental molecules exists that effectively deplete the intrinsic electron density in MoS₂. Vice versa, a high laser power diminishes the amount of physisorbed molecules (laser cleaning) resulting in a reduction of the charge transfer from MoS₂ and a large electron density within the 2D crystal.

In a steady state illumination the amount of physisorbed molecules is given by laser cleaning and physisorption rates. Whereas the physisorption rate is fixed for a specific sample and its environment, the laser cleaning rate depends on the light intensity. In this way, we explain the tunability of the laser power induced change in the charge carrier density. Differences between the

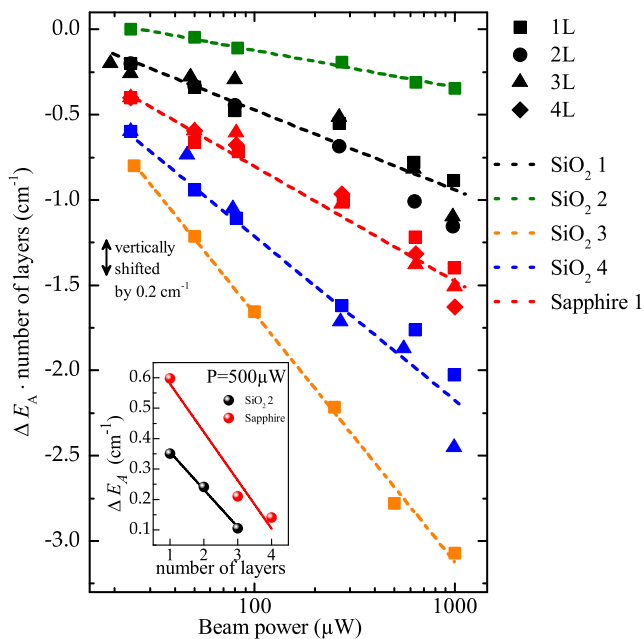


FIG. 4. Laser power dependent energy shift ΔE_A of the A_{1g} phonon mode (relative to the A_{1g} mode energy at $P = 25\mu\text{W}$) for different samples and number of layers in ambient conditions. The deduced energy shift ΔE_A is multiplied by the number of layers. The traces are shifted vertically by 0.2 cm^{-1} for clarity. Inset: ΔE_A vs number of layers for to sample at an laser power of $P = 500\text{ }\mu\text{W}$.

individual samples are expected to be caused by crystal defects such as sulfur vacancies in the MoS_2 lattice[14] or ripples acting as attractive sites for physisorption of environmental molecules. The used substrate materials seem to play an inferior role compared to the statistical

variation from flake to flake exfoliated from the identical bulk crystal.

Fig. 4 shows the laser power dependent shift of the A_{1g} phonon mode energy ΔE_A relative to the mode energy at $P = 25\mu\text{W}$ for different flakes consisting of mono- and few-layer parts. Intriguingly, we find that ΔE_A scales linearly with the inverse number of layers. In Fig. 4, the shift of the A_1 mode energy multiplied by the number of layers ($\Delta E_A \times \text{number of layers}$) is plotted vs. the laser power for 6 samples. The scaling with respect to the number of layers [inst Fig. 4] reveals that the phonon-renormalization has a similar influence on the A_{1g} mode energy for mono-, bi-, tri- and four-layer MoS_2 under the assumption that free charge carriers are delocalized and freely distributed over all individual basal planes. The same proportionality is observable for electrostatically induced changes in the electron density for MoS_2 mono- and bi-layer flakes [Fig. 3].

In summary, we show that the charge carrier density in MoS_2 -devices in ambient conditions is precisely tunable by the light intensity. This photogating effect is studied by Raman spectroscopy by the sensitivity of the A_{1g} phonon mode to the charge carrier density. The photogating is quantified from comparison with gate-voltage dependent measurements on field effect devices. We further conclude that the charge carrier density is homogeneously distributed over the basal planes for up to 4 layers. Our study reveals that the photogating can be assigned to the light induced removal of physisorbed molecules acting as molecular gates. This effect facilitates to reversibly modify the interfacial properties of optoelectronic MoS_2 devices without the need for electrical contacts.

We acknowledge fruitful discussions with Joel W. Ager and financial support by the DFG via excellence cluster Nanosystems Initiative Munich (NIM) and project Ho 3324/8-1 as well as BaCaTec.

-
- [1] Q. H. Wang, K. Kalantar-Zadeh, A. Kis, J. N. Coleman, and M. S. Strano, *Nature Nanotech.* **7**, 699 (2012).
- [2] B. Radisavljevic, A. Radenovic, J. Brivio, V. Giacometti, and A. Kis, *Nature Nanotech.* **6**, 147 (2011).
- [3] K. F. Mak, C. Lee, J. Hone, J. Shan, and T. F. Heinz, *Phys. Rev. Lett.* **105**, 136805 (2010).
- [4] Z. Yin, H. Li, H. Li, L. Jiang, Y. Shi, Y. Sun, G. Lu, Q. Zhang, X. Chen, and H. Zhang, *ACS Nano* **6**, 74 (2012).
- [5] O. Lopez-Sanchez, D. Lembke, M. Kayci, A. Radenovic, and A. Kis, *Nature Nanotech.* **8**, 497 (2013).
- [6] X. Xu, W. Yao, Di Xiao, and T. F. Heinz, *Nature Phys.* **10**, 343 (2014).
- [7] M.-L. Tsai, S.-H. Su, J.-K. Chang, D.-S. Tsai, C.-H. Chen, C.-I. Wu, L.-J. Li, L.-J. Chen, and J.-H. He, *ACS Nano* **8**, 8317 (2014).
- [8] D. J. Late, Y.-K. Huang, B. Liu, J. Acharya, S. N. Shirodkar, J. Luo, A. Yan, D. Charles, U. V. Waghmare, V. P. Dravid, and Rao, *C N R, ACS Nano* **7**, 4879 (2013).
- [9] M. Bernardi, M. Palummo, and J. C. Grossman, *Nano Lett.* **13**, 3664 (2013).
- [10] Y. Li, C.-Y. Xu, P. Hu, and L. Zhen, *ACS Nano* **7**, 7795 (2013).
- [11] M. Buscema, G. A. Steele, van der Zant, Herre S. J., and A. Castellanos-Gomez, *Nano Research* **7**, 561 (2014).
- [12] S. Tongay, J. Zhou, C. Ataca, J. Liu, J. S. Kang, T. S. Matthews, L. You, J. Li, J. C. Grossman, and J. Wu, *Nano Lett.* **13**, 2831 (2013).
- [13] N. Mao, Y. Chen, D. Liu, J. Zhang, and L. Xie, *Small* **9**, 1312 (2013).
- [14] H. Nan, Z. Wang, W. Wang, Z. Liang, Y. Lu, Q. Chen, D. He, P. Tan, F. Miao, X. Wang, J. Wang, and Z. Ni, *ACS Nano* **8**, 5738 (2014).
- [15] Q. Yue, Z. Shao, S. Chang, and J. Li, *Nanoscale Research Letters* **8**, 425 (2013).
- [16] S. Najmaei, X. Zou, D. Er, J. Li, Z. Jin, W. Gao, Q. Zhang, S. Park, L. Ge, S. Lei, J. Kono, V. B. Shenoy, B. I. Yakobson, A. George, P. M. Ajayan, and J. Lou,

- Nano Lett. **14**, 1354 (2014).
- [17] M. A. Pimenta, E. del Corro, B. R. Carvalho, C. Fantini, and L. M. Malard, *Acc. Chem. Res.* **48**, 41 (2015).
- [18] C. Lee, H. Yan, L. E. Brus, T. F. Heinz, J. Hone, and S. Ryu, *ACS Nano* **4**, 2695 (2010).
- [19] G. Plechinger, S. Heydrich, J. Eroms, D. Weiss, C. Schüller, and T. Korn, *Appl. Phys. Lett.* **101**, 101906 (2012).
- [20] C. Rice, R. Young, R. Zan, U. Bangert, D. Wolverson, T. Georgiou, R. Jalil, and K. Novoselov, *Phys. Rev. B* **87** (2013).
- [21] H. J. Conley, B. Wang, J. I. Ziegler, R. F. Haglund, S. T. Pantelides, and K. I. Bolotin, *Nano Lett.* **13**, 3626 (2013).
- [22] N. A. Lanzillo, A. Glen Birdwell, M. Amani, F. J. Crowne, P. B. Shah, S. Najmaei, Z. Liu, P. M. Ajayan, J. Lou, M. Dubey, S. K. Nayak, and T. P. O'Regan, *Appl. Phys. Lett.* **103**, 093102 (2013).
- [23] B. Chakraborty, A. Bera, Muthu, D. V. S., S. Bhowmick, U. V. Waghmare, and A. K. Sood, *Phys. Rev. B* **85**, 161403(R) (2012).
- [24] A. Das, S. Pisana, B. Chakraborty, S. Piscanec, S. K. Saha, U. V. Waghmare, K. S. Novoselov, H. R. Krishnamurthy, A. K. Geim, A. C. Ferrari, and A. K. Sood, *Nature Nanotech.* **3**, 210 (2008).